

Supplementary Information

Spin Cross-Over (SCO) Anionic Fe(II) Complexes Based on the Tripodal Ligand Tris(2-pyridyl)ethoxymethane

Emmelyne Cuza ¹, Samia Benmansour ², Nathalie Cosquer ¹, Françoise Conan ¹, Sébastien Pillet ³, Carlos J. Gómez-García ² and Smail Triki ^{1,*}

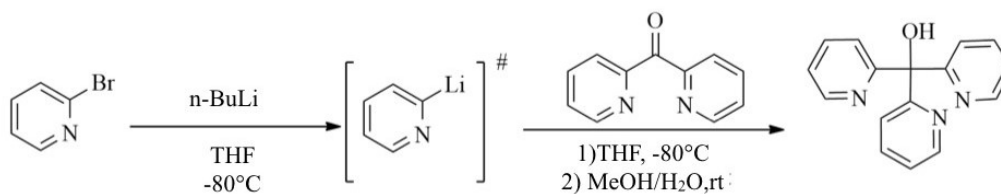
¹ Univ Brest, CNRS, CEMCA, 6 Avenue Le Gorgeu, C.S. 93837 - 29238 Brest Cedex 3, France;
emmelyne.cuza@univ-brest.fr (E.C.); nathalie.cosquer@univ-brest.fr (N.C.); Francoise.Conan@univ-brest.fr (F.C.)

² Instituto de Ciencia Molecular (ICMol). Departamento de Química Inorgánica. Universidad de Valencia.
C/Catedrático José Beltrán 2. 46980 Paterna, Spain;
Sam.Ben@uv.es (S.B.); Carlos.Gomez@uv.es (C.J.G.G)

³ Laboratoire de Cristallographie, Résonance Magnétique et Modélisations, UMR 7036, Boulevard des
aiguillettes, BP239 54506 Vandoeuvre-les-Nancy, France
sebastien.pillet@univ-lorraine.fr (S.P.)

* Correspondence: smail.triki@univ-brest.fr; Tel.: +33-298-016-146

1 - Chemical syntheses and spectroscopic characterisations



Scheme S1. Synthesis of tris(pyridin-2-yl)methanol (py₃C-OH)

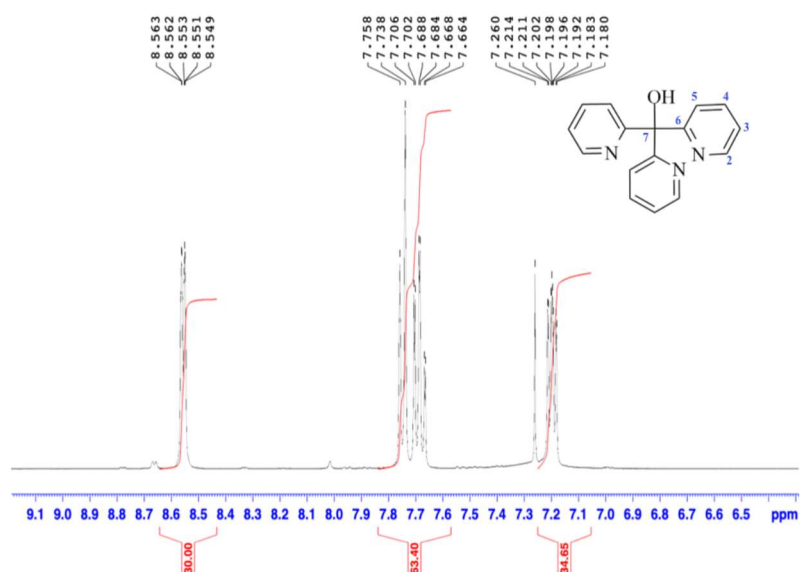


Figure S1. ¹H NMR (CDCl₃, 400 MHz, δ (ppm)) of py₃C-OH at 25 °C: 7.20 (3H, CH aromatic, q, 3JH-H= 5 Hz, H3), 7.68 (3H, CH aromatic, td, H4), 7.75 (3H, CH aromatic, q, 3JH-H= 8 Hz, H5), 8.46 (3H, CH aromatic, 3JH-H= 5 Hz, td, H2).

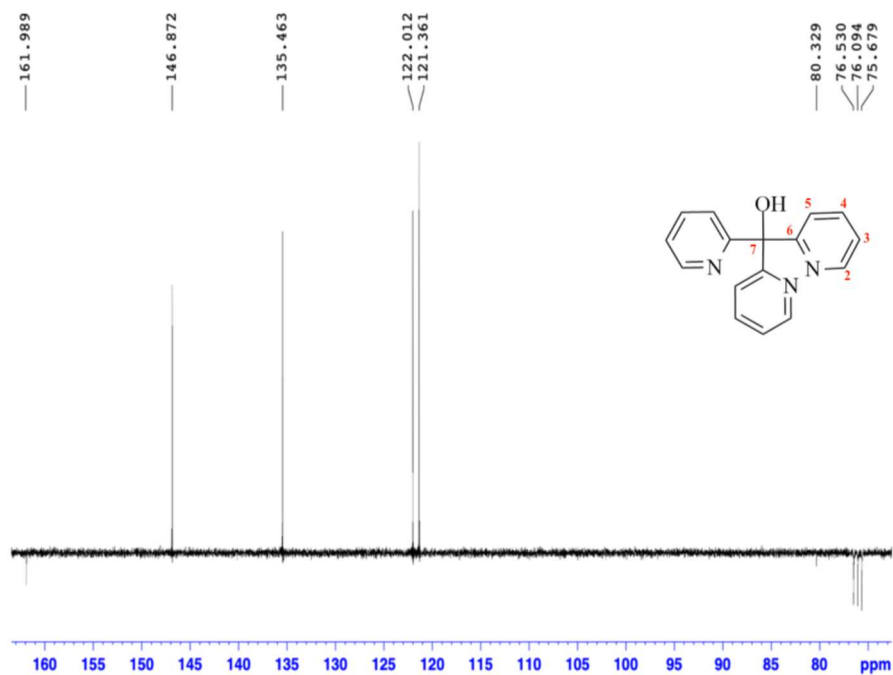


Figure S2. ¹³C NMR (CDCl₃, 75 MHz, δ (ppm)) of py₃C-OH at 25 °C: 81.27 (C7), 121.36 (C3), 122.01 (C5) 135.46 (C4), 146.87 (C2), 161.99 (C6).

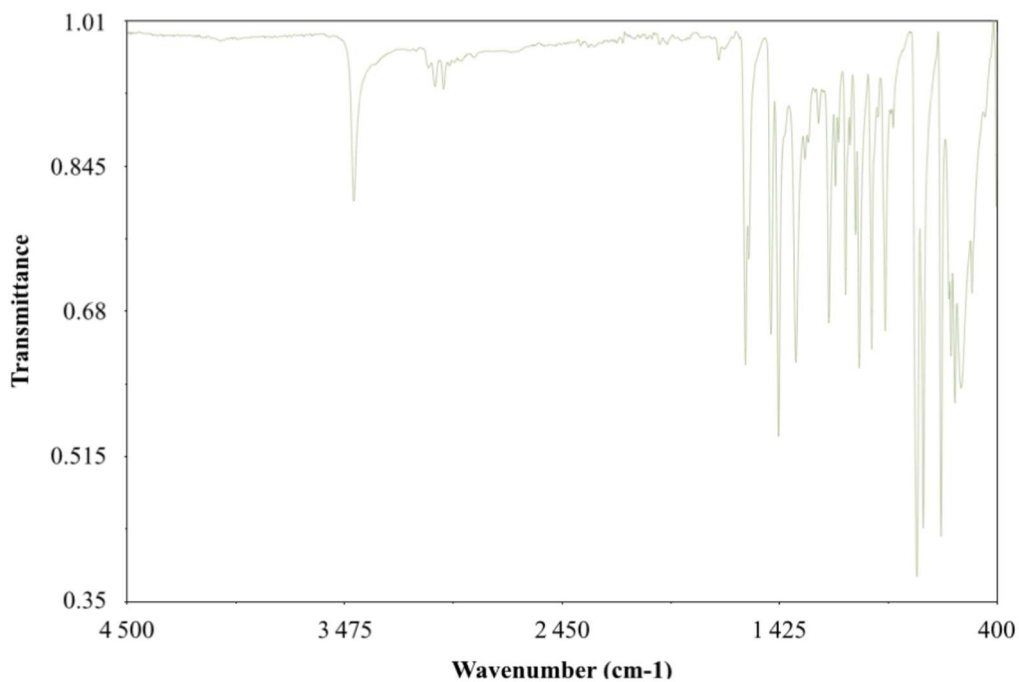
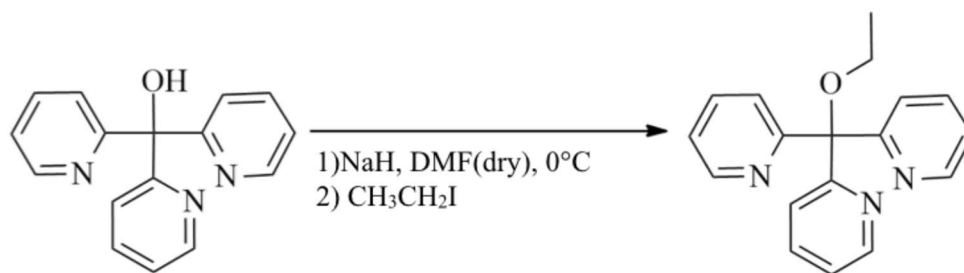


Figure S3. IR spectrum of py₃C-OH at 25 °C (cm⁻¹): 456 (w), 517 (m); 569 (s); 598 (m) 627 (w), 663 (s); 748 (s), 778 (s), 891 (w) 928 (m), 962 (w), 996 (m), 1051 (m), 1115 (m), 1193 (m), 1242 (w), 1290 (w), 1306 (w), 1349 (s), 1430 (s), 1465 (m), 1570 (m), 1585 (s), 1743 (w), 2979 (w), 3008 (w), 3047 (w), 3432 (m).



Scheme S2. Synthesis of tris(pyridin-2-yl)ethoxymethane (py₃C-OEt).

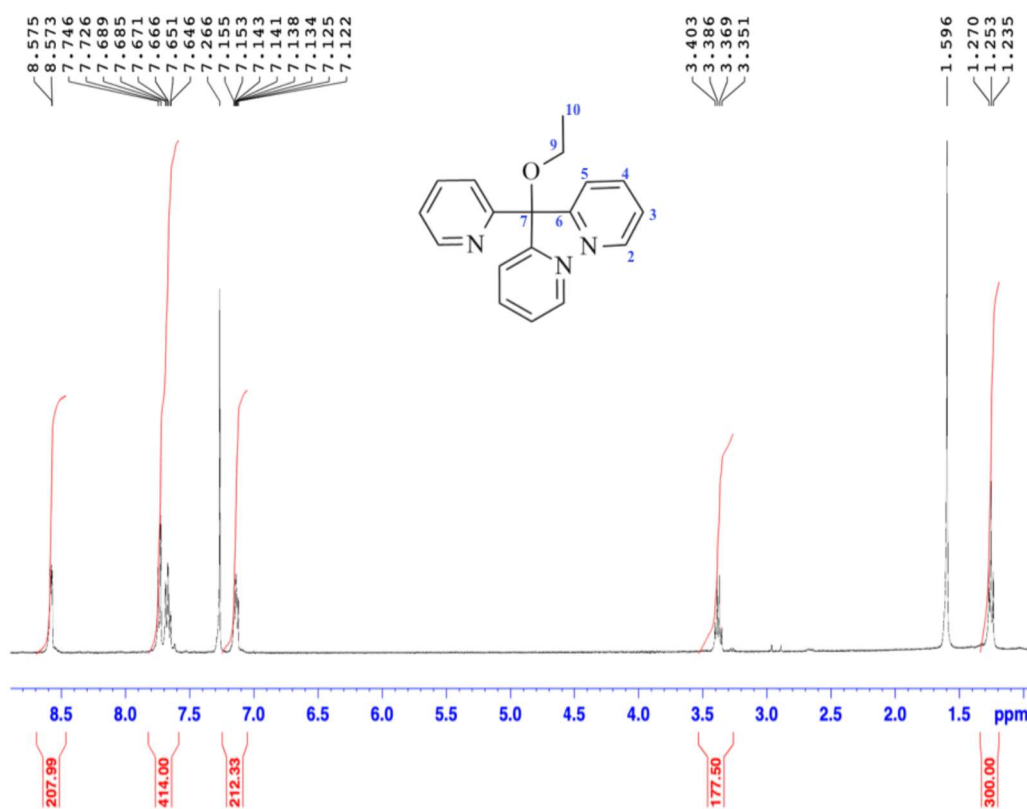


Figure S4. ¹H NMR (CDCl₃, 400 MHz, δ (ppm)) of py₃C-OEt at 25 C: 1.24 (3H, CH₃, t, 3J_{H-H}= 7,2 Hz, H10), 3.37 (2H, CH₂, q, 3J_{H-H}= 7,2Hz, H9), 7.13 (3H, CH aromatic ring, q, 3J_{H-H}= 8 Hz, H3), 7.65 (3H, CH aromatic ring, q, 3J_{H-H}= 8 Hz, H5), 7.73 (3H, CH aromatic ring, d, 3J_{H-H}= 8 Hz, H4), 8.57 (2H, CH aromatic ring, d, 3J_{H-H}= 4,8 Hz, H2).

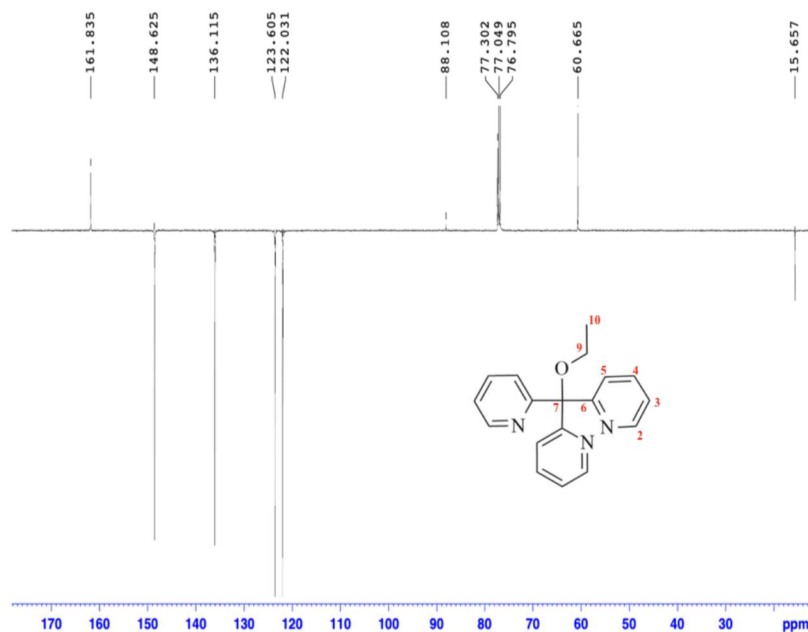


Figure S5. ^{13}C NMR (CDCl_3 , 125 MHz, δ (ppm)) of $\text{py}_3\text{C-OEt}$ at 25°C: 15.56 (C10), 60.67 (C9), 88.11 (C7), 122.03 (C3), 123.61 (C5) 136.16 (C4), 148.63 (C2), 161.84 (C6).

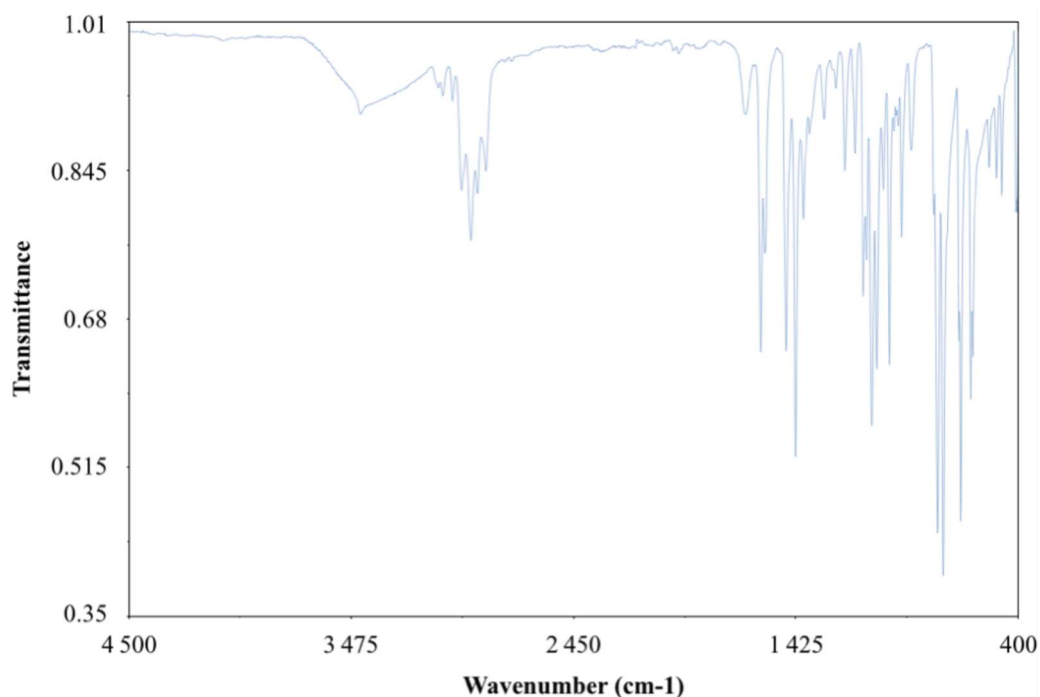


Figure S6. IR of $\text{py}_3\text{C-OEt}$ at 25 °C (cm^{-1}): 476 (w), 500 (w), 534 (w), 610 (m), 619 (s), 665 (s), 673 (m), 745 (s), 771 (s), 789 (w), 893 (w & l), 937 (m), 953 (w), 993 (s), 1021 (m), 1051 (s), 1074 (s), 1098 (m), 1114 (m), 1152 (w), 1199 (w), 1240 (w), 1293 (w), 1361 (w), 1390 (m), 1426 (s), 1469 (s), 1567 (m), 1586 (s), 1658 (br), 2854 (w), 2893 (w), 2922 (m), 2967 (w), 3009 (w), 3053 (w).

2 – Structural characterisations

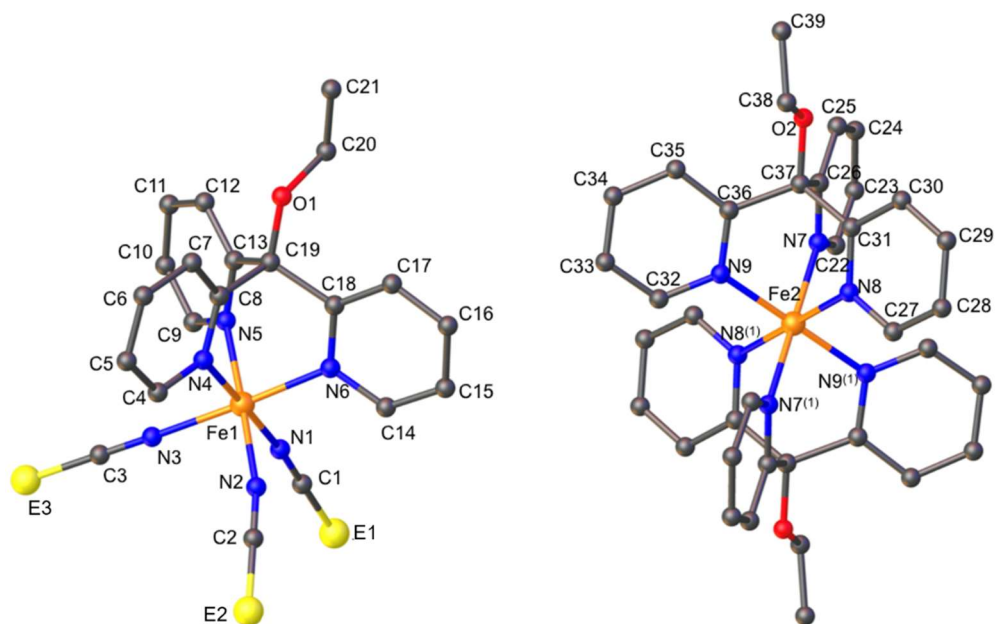




Figure S7. Molecular structure of **1-2** showing the asymmetric unit and the Fe(II) environments of the anionic ($[\text{Fe}(\text{py}_3\text{C-OEt})(\text{NCE})_3]^-$) and cationic ($[\text{Fe}(\text{py}_3\text{C-OEt})_2]^{2+}$) moieties. Hydrogen atoms are omitted for the sake of clarity. Codes of equivalent position: (1) = $-x, -y, -z$.

Table S1. Crystal data and structural refinement parameters for complexes [Fe(py₃C-OEt)₂][Fe(py₃C-OEt)(NCE)₃]₂·2CH₃CN (E = S (**1**), BH₃ (**2**)).

Complex	1		2
Temperature (K)	293	100	200
Color	 Orange	 Red	Red
Formula	C ₈₂ H ₇₄ Fe ₃ N ₂₀ O ₄ S ₆		C ₈₂ H ₉₂ Fe ₃ N ₂₀ O ₄ B ₆
Radiation	MoKα (λ = 0.71073)		MoKα (λ = 0.71073)
M (g·mol ⁻¹)	1763.52		1654.16
Cryst. syst / Space group	Triclinic / <i>P</i> -1		Triclinic / <i>P</i> -1
a (Å)	11.6683(5)	11.432(5)	11.6827(8)
b (Å)	11.9026(7)	11.829(5)	12.0204(10)
c (Å)	17.1711(9)	16.857(5)	16.9162(11)
α (°)	78.192(5)	78.072(5)	78.389(6)
β (°)	88.279(4)	88.037(5)	87.805(6)
γ (°)	66.544(5)	65.879(5)	65.767(7)
Volume (Å ³)	2137.9(2)	2032.4(14)	2119.3(3)
Z	1		1
ρ _{calc} (g/cm ⁻³)	1.370	1.441	1.296
μ (mm ⁻¹)	0.710	0.747	0.568
F(000)	912.0	912.0	864.0
2θ range (°)	6.834 - 58.856	6.527 - 58.824	6.508 to 58.484
Reflections collected	18918	26672	15809
Independent reflections / R _{int}	9830 / 0.0458	9534 / 0.0722	9657 / 0.0701
Goodness-of-fit on F ²	1.028	1.066	0.997
R ₁ / wR ₂	0.0692 / 0.1697	0.0605 / 0.1476	0.0823 / 0.2031
Δρ _{max} /min (e·Å ⁻³)	0.892/-0.703	2.11/-1.047	1.177/-1.490
Data/restraints/parameters	5988 / 56 / 523	6916 / 58 / 523	5051 / 74 / 550

$${}^a R_1 = \sum |F_o - F_c| / F_o, \quad {}^b wR_2 = \{w(F_o^2 - F_c^2)^2\} / \{wF_o^2\}^{1/2}, \quad {}^c \text{Goof} = \{w(F_o^2 - F_c^2)^2\} / (N_{\text{obs}} - N_{\text{var}})^{1/2}$$

Table S2. Bond lengths and bond angles of compounds **1** and **2**.

Compounds	1	2	
	293 K	100 K	200 K
Fe1-N1	2.083(4)	1.949(3)	1.944(4)
Fe1-N2	2.086(4)	1.956(3)	1.954(4)
Fe1-N3	2.110(4)	1.965(3)	1.943(5)
Fe1-N4	2.237(3)	1.987(3)	1.978(4)
Fe1-N5	2.180(3)	1.948(3)	1.943(4)
Fe1-N6	2.191(3)	1.952(3)	1.945(4)
Fe2-N7	2.003(3)	1.989(3)	1.998(4)
Fe2-N8	1.962(3)	1.960(3)	1.947(4)
Fe2-N9	1.957(3)	1.954(3)	1.963(4)
N1-Fe1-N2	93.81(16)	89.10(12)	89.43(17)
N1-Fe1-N3	93.57(16)	89.71(12)	88.76(17)
N1-Fe1-N4	174.87(13)	178.91(11)	179.06(17)
N1-Fe1-N6	93.55(14)	92.32(12)	92.52(17)
N2-Fe1-N3	94.83(15)	89.14(11)	88.69(18)
N2-Fe1-N4	89.62(13)	89.90(11)	89.90(17)
N3-Fe1-N4	89.94(13)	89.84(12)	90.56(17)
N5-Fe1-N1	94.34(14)	92.92(11)	92.47(17)
N5-Fe1-N2	170.20(13)	177.71(12)	177.47(17)
N5-Fe1-N3	90.09(14)	89.79(11)	93.02(18)
N5-Fe1-N4	81.90(11)	88.07(11)	88.22(16)
N5-Fe1-N6	79.16(12)	88.58(11)	88.48(17)
N6-Fe1-N2	94.90(14)	92.41(11)	89.78(17)
N6-Fe1-N3	167.52(13)	177.46(12)	177.99(17)
N6-Fe1-N4	82.34(11)	88.16(11)	88.15(16)

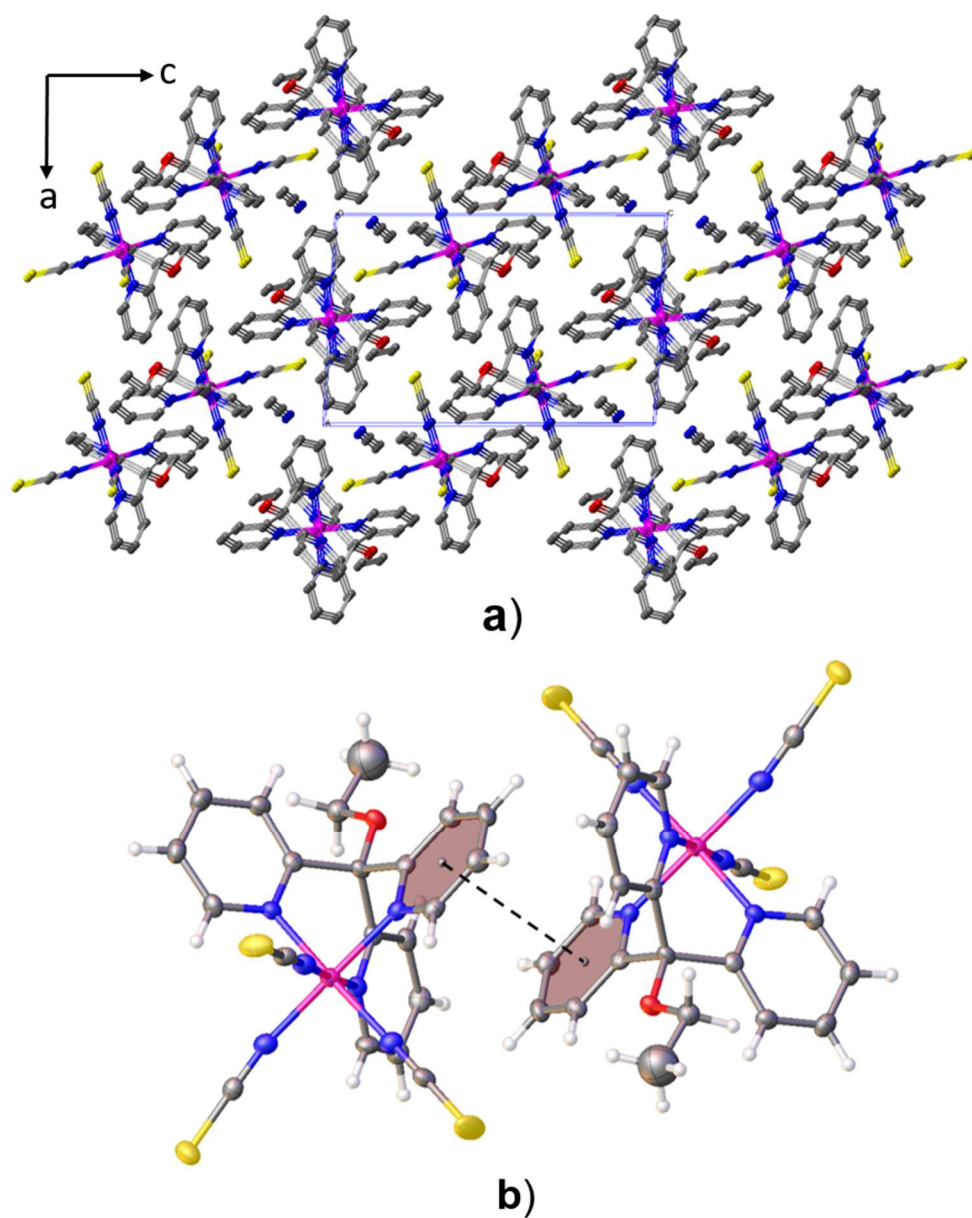


Figure S8. Projection of the crystal packing in the *ac* plane (a) and π - π contact motif (b) of **1** (similar in **2**)

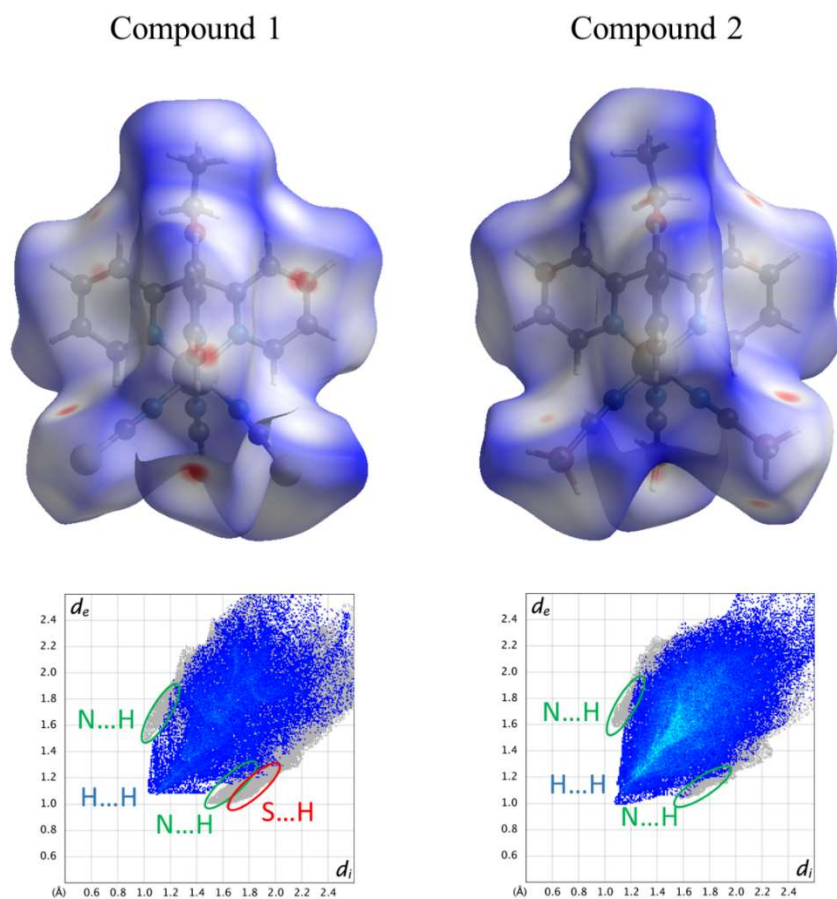


Figure S9. 3D Hirshfeld surface maps and fingerprint plots of the intermolecular interactions around the $[\text{Fe}(\text{py}_3\text{C-OEt})(\text{NCE})_3]^-$ anions for compounds **1** and **2**.

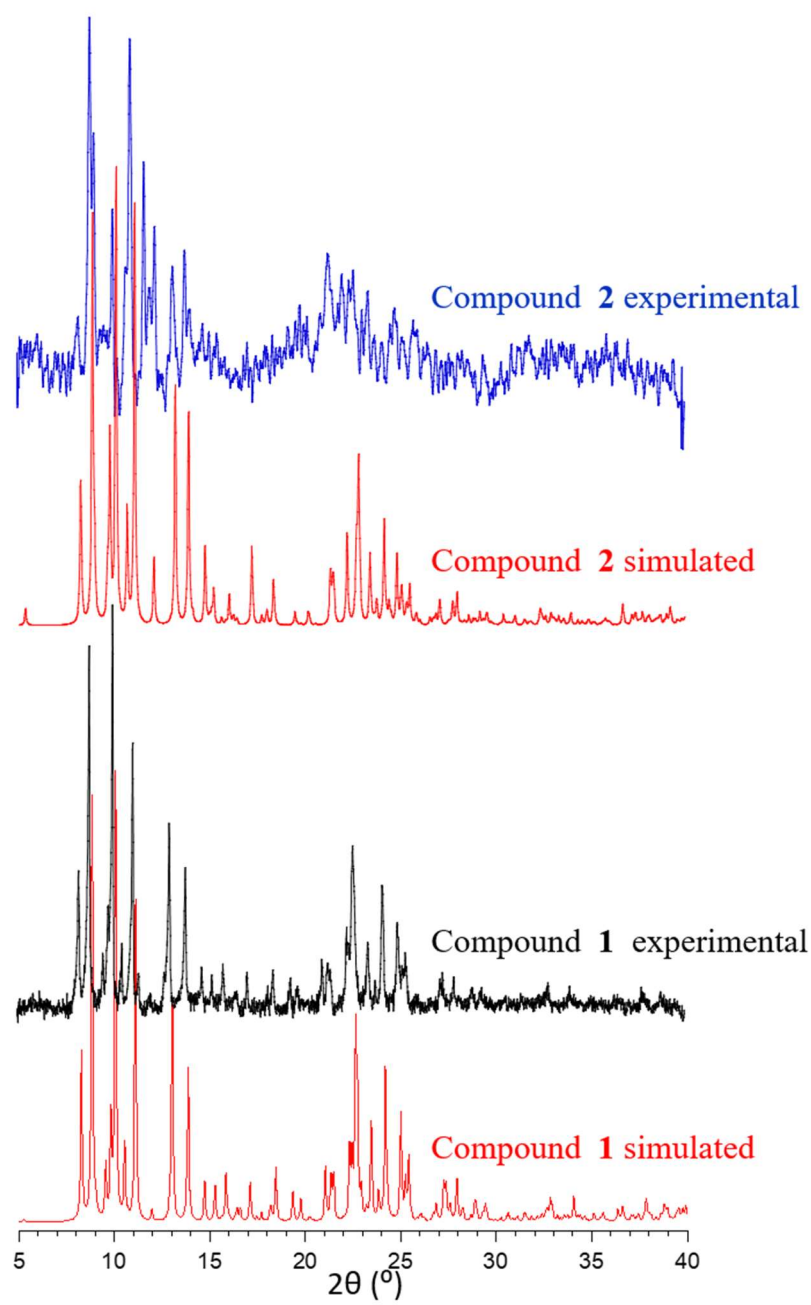


Figure S10. Experimental and simulated XRPD patterns for compounds **1** and **2**.